Heat treatment control of Ag–$Bi_2Sr_2CaCu_2O_x$ multifilamentary round wire: investigation of time in the melt

2011 Supercond. Sci. Technol. 24 115009

(http://iopscience.iop.org/0953-2048/24/11/115009)

Supercond. Sci. Technol. **24** (2011) 115009 (8pp) doi:10.1088/0953-2048/24/11/115009

Heat treatment control of $Ag–Bi_2Sr_2CaCu_2O_x$ multifilamentary round wire: investigation of time in the melt

Tengming Shen[1,2,4], Jianyi Jiang[1], Fumitake Kametani[1], Ulf P Trociewitz[1], David C Larbalestier[1,3] and Eric E Hellstrom[1,3]

[1] Applied Superconductivity Center, National High Magnetic Field Laboratory, Florida State University, Tallahassee, FL 32310, USA
[2] Department of Electrical and Computer Engineering, FAMU-FSU College of Engineering, Florida State University, Tallahassee, FL 32310, USA
[3] Department of Mechanical Engineering, FAMU-FSU College of Engineering, Florida State University, Tallahassee, FL 32310, USA

Received 25 April 2011, in final form 6 September 2011
Published 17 October 2011
Online at stacks.iop.org/SUST/24/115009

Abstract

It is well known that the critical current density J_c of Ag-sheathed $Bi_2Sr_2CaCu_2O_x$ (2212) varies strongly with heat treatment details, particularly the maximum processing temperature T_{max}, but the mechanism for such J_c variations and how the processing window can be widened remain unknown. We systematically measured the J_c and electromagnetic properties of a powder-in-tube Ag-sheathed multifilamentary $Bi_2Sr_2CaCu_2O_x$ (2212) round wire processed with the maximum processing temperature T_{max} ranging from 887 to 900 °C and the time at the maximum temperature t_{max} from 0 to 3 h using three representative heat treatment schedules. We found that J_c correlates weakly to T_{max}, but it correlates strongly to the time in the melt t_{melt}, a processing parameter that has not been explicitly considered before. J_c is rather insensitive to T_{max} in the temperature range 887–900 °C and the true cause of J_c declining with high T_{max} appears to be the long t_{melt} that leads to collapse of filament structure. By tuning t_{melt} we were able to widen the T_{max} window to 10 °C. The J_c–t_{melt} correlation, as well as quench studies, indicate that J_c is controlled by complex diffusion processes occurring in the melt (filament bonding, bubble agglomeration, and perhaps Cu loss). Our findings highlight t_{melt} as an important processing parameter for optimizing J_c and may serve as a general guide for heat treating 2212 coils.

(Some figures in this article are in colour only in the electronic version)

1. Introduction

Ag-sheathed multifilamentary $Bi_2Sr_2CaCu_2O_x$ (2212) round wire exhibits a high critical current density J_c of 10^5 A cm^{-2} (at 4.2 K up to 45 T) [1] and a high irreversibility field exceeding 100 T. Thus it has great potential for generating high magnetic fields exceeding the maximum of about 22 T attainable with Nb_3Sn, enabling applications that range from >1 GHz NMR spectroscopy [2] to high-energy particle colliders [3]. Long-length 2212 round wires that enable Rutherford cables are fabricated using a powder-in-tube (PIT) approach by two US companies (Oxford Superconducting Technology (OST) in New Jersey and Supercon in Massachusetts) [1, 4] and SWCC Showa Holdings Co. in Japan [5]. Recently, solenoid inserts wound from 2212 round wire reached 32 T in a resistive magnetic background field of 31 T [6] and achieved 22.5 T [7] in an all-superconducting magnet. Racetrack coils have been successfully fabricated from 2212 Rutherford cables [8, 9]. The solenoid and racetrack coils were made using a wind-and-react approach.

[4] Present address: Fermi National Accelerator Lab, Batavia, IL 60510, USA.

A partial melt heat treatment [10] is widely used to produce high J_c in a 2212 conductor but heat treating 2212 coils using this approach is seen as being difficult [11, 12], mainly because high J_c is often achieved only in a maximum processing temperature T_{max} window (where >90% of optimum J_c is achieved) that is often 2–4 °C wide [13]. For many 2212 conductors, including Ag-sheathed dip-coated tapes [14, 15], tape-casting thin films on Ag [14, 16] and other substrates, and PIT multifilamentary round wires [17, 18], J_c is almost zero below a threshold $T_{max} \sim$ 882–884 °C and peaks around an optimum $T_{max} \sim$ 887 °C [14]. When T_{max} is raised beyond the optimum T_{max}, J_c decreases by varying amounts with increasing T_{max}.

Work by Nexans and OST [18–20] has shown that the T_{max} window can be as wide as 12 °C (J_c decreased by 25% for T_{max} ranging from 892 to 904 °C [19]). They pointed out that broadening the window was complicated and depended on the composition and phase-state of the 2212, T_{max}, t_{max} (time at the maximum temperature), and the cooling and heating rates, as well as other details of the heat treatment. It was not easy to transfer their findings to other wires to widen the T_{max} window. When we began this study, we were processing wires made by OST with Nexans powder and were finding rather narrow J_c–T_{max} behavior. Our results did not dissuade our collaborators at Brookhaven National Lab, Lawrence Berkeley National Lab, and Fermi National Accelerator Lab, who are interested in building very-high-field 2212 magnets, from their belief that it would be very difficult to control the temperature to heat treat large coils. Thus our overall goal in this study was to understand what occurs at high temperature that is responsible for the very narrow J_c–T_{max} window often reported in the literature and to use this understanding to increase the width of processing window.

Many mechanisms have been proposed to explain why J_c decreases when raising T_{max} above the optimum T_{max}. It is suggested that increasing T_{max} causes phases in the melt to change their composition, causes excessive grain growth of the crystalline, non-superconducting phases in the melt that are preferred to be small, or causes the formation of very large bubbles (pores) [14, 16]. All these explanations point to temperature as the primary source of the problem and some mention that increasing T_{max} increases the time at high temperature, which can allow more growth of non-superconducting phases in the melt.

Melting 2212 powder has been shown to be critical for developing J_c, as evidenced by J_c being ~0 A mm^{-2} in wires processed with T_{max} below the 2212 melting temperature [17, 21]. We wondered what mechanism is responsible for the dramatic decrease in J_c when T_{max} is increased by just a few degrees after exceeding the optimum T_{max}. In one case J_c decreased by 40% on increasing T_{max} from 885 to 890 °C [22]. J_c is normally plotted as a function of T_{max} when optimizing a heat treatment to maximize J_c. But we wondered if T_{max} was the only critical processing variable because the increase in thermal energy between 885 and 890 °C is only 0.43%, as given by RT, where R is the gas constant and T is temperature. Further, for a thermally activated process like diffusion, increasing the temperature from 885 to 890 °C only increases the activated energy component of the process by 4.6% if the activation energy is 100 kJ mol^{-1} and 9.4% if the activation energy is 200 kJ mol^{-1}. It did not seem plausible that these small changes in thermal energy and energy component could explain the large changes in J_c.

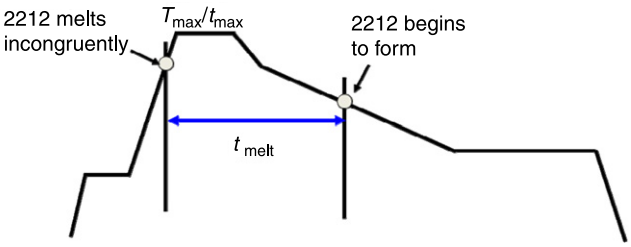

Figure 1. A typical heat treatment schedule used for 2212 wire. t_{melt} is the time between when the 2212 phase melts incongruently on heating (884 °C) and when the 2212 phase begins to form from the melt on cooling (872 °C). In quench experiments where the sample is quenched from $T >$ 872 °C, t_{melt} is the time from 884 °C on heating until the sample is quenched.

Another important factor for kinetics is time. Possible effects from increasing the length of time at elevated temperature when heat treating 2212 have been alluded to in previous studies and time in the partial melt state was mentioned, but not defined, by Matsumoto *et al* [17]. However, time in the melt state had not been studied as a processing variable affecting the electromagnetic behavior of 2212 conductors. In this study we explicitly investigated the effect that time at elevated temperature has on J_c. Specifically, we investigated J_c as a function of time in the melt, t_{melt}, which we define as the time from when the 2212 phase melts on heating until it begins to reform on cooling. This is shown schematically in figure 1. In previous quench studies [23, 24], we found that in the wire we used in the present study 2212 melts at 884 °C and the 2212 phase begins to form on cooling at 872 °C (when the cooling rate during solidification is 2.5 °C h^{-1}), so t_{melt} is defined as the time between these temperatures.

For this study we designed three different heat treatment schedules, which are shown in figure 2. The designations for these heat treatments given in figure 2 are LT for long time in the melt, ST for short time in the melt, and STD for standard heat treatment, which is what we normally use to heat treat 2212 conductors at the National High Magnetic Field Lab. Each heat treatment has the same heating rate when 2212 melts and the same cooling rate when the 2212 nucleates on cooling, and a set of experiments used the same T_{max} and t_{max}. The differences in the heat treatments were how they cooled the samples from T_{max} to 874 °C. The heat treatments had the same cooling rate from 874 through 872 °C where 2212 began to nucleate and were identical from 872 °C to room temperature. In a previous study [23], we found that the cooling rate during 2212 solidification strongly affects grain growth and J_c, and that most of the 2212 grain growth has finished by 860 °C for wires cooled at 2.5 °C h^{-1}. Each of the heat treatment schedules gives a different t_{melt} for the same T_{max} and t_{max}. For a given T_{max} and t_{max}, t_{melt} is longest for heat treatment LT and shortest for ST.

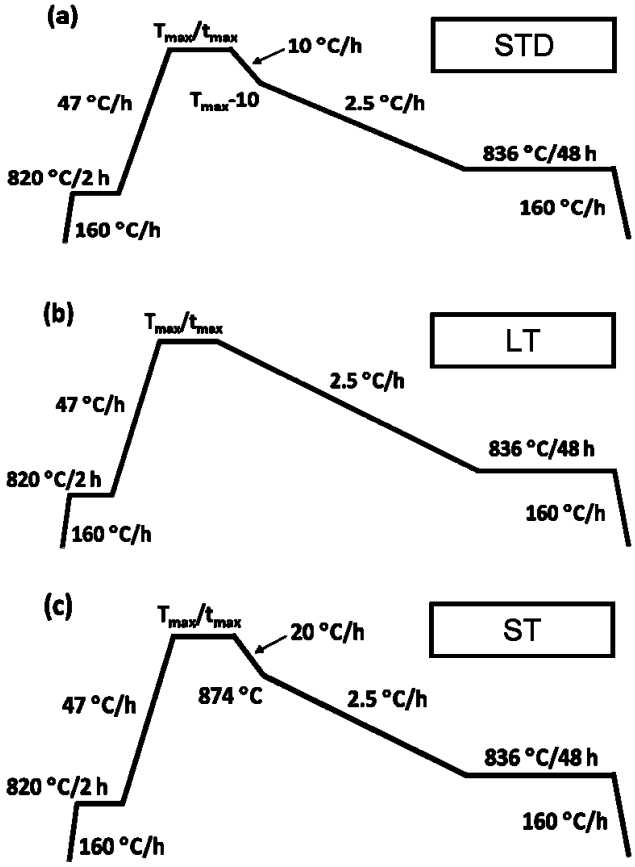

Figure 2. Schematic diagram of the heat treatment schedules used in the study: (a) standard melt processing (called STD) used at the National High Magnetic Field Laboratory; (b) a melt processing schedule that gives a long t_{melt}, called LT; and (c) a melt processing schedule that gives a short t_{melt}, called ST. For example, for $T_{max} = 894\,^{\circ}C$ and $t_{max} = 0.2$ h, t_{melt} is 9.2 h for LT, 6.6 h for STD, and 1.7 h for ST. t_{melt} depends on T_{max}, t_{max}, the heating rate to T_{max}, and the cooling rates in the melt, so it can be reproducibly 'tuned' by suitable choices of heating and cooling rates, T_{max}, and t_{max}.

The results show that J_c decreases linearly with increasing t_{melt} when $t_{melt} \gtrsim 2.5$ h. We observed the filament structure, phase assemblage in the melt, and growth of 2212 grains from the melt on increasing t_{melt} from 0.2 to 48 h. The J_c decreases with increasing t_{melt} ($\gtrsim$2.5 h) because with increasing t_{melt} more filaments bond together due to liquid and Ag transport so the filaments become distorted and discontinuous, small bubbles continue to agglomerate into larger bubbles that block the filaments, and Cu may be lost from the 2212 melt. Identifying the J_c–t_{melt} relationship and understanding what occurs in the melt allow design of new heat treatment for coils.

2. Experimental procedures

We used Ag-sheathed 2212 multifilamentary round wire fabricated by Oxford Superconducting Technology using the PIT technique. It had a double-restack architecture with seven bundles each with 85 filaments. The wire, which was ~1.06 mm in diameter, contained filaments that were ~20 μm in diameter and spaced ~15 μm apart. Its outer sheath was a Ag–Mg alloy. The Ag to superconductor volume ratio was 3. The overall composition of the precursor powder was $Bi_{2.17}Sr_{1.94}Ca_{0.89}Cu_{2.00}O_x$ (Nexans Superconductor) [20].

The heat treatment schedules used in this study, shown in figure 2, were selected as representative of processes that are currently in use or have been used in the past [15, 16, 18, 19, 23–25]. T_{max} was varied from 887 to 900 °C and t_{max} was varied from 0.2 to 3 h for these studies. Samples 4 cm long were heat treated in a vertical tube furnace following the heat treatment schedules shown in figure 2 in 1 bar flowing O_2. The ends of the wires were mechanically sealed to prevent 2212 liquid from leaking out during the heat treatment. Samples were quenched from high-temperature into room-temperature brine [23, 26] to observe the microstructure during the heat treatment. Some samples were fully processed in the same furnace without being quenched.

The quenched and fully-processed wires were dry polished using a series of SiC papers with decreasing grit sizes. The final polishing was conducted in a 50 nm alumina suspension in ethanol using an automatic vibratory polisher (Vibramet, Buehler), which gently removes Ag that was smeared into pores in previous polishing steps. The microstructure of longitudinal and transverse sections of polished samples was examined using a scanning electron microscope (Zeiss 1540 ESB). X-ray energy dispersive spectroscopy was used to examine the phase chemistry.

Transport critical current I_c was measured using the four-probe method with a 1 μV cm^{-1} criterion at 4.2 K in a 5 T magnetic field applied perpendicular to the wire axis. The area used to calculate J_c was the oxide filament area determined from SEM cross-sections of unreacted wires using digital image analysis (ImageJ, NIH). Reported J_c values are averages of four samples heat treated identically. There was very little scatter of J_c in each set of four wires. After measuring I_c, ~5 mm long samples were cut from these wires for further electromagnetic characterization and microstructure evaluation. Magnetic hysteresis was measured using an Oxford Instruments 14 T vibrating sample magnetometer from 4.2 up to 20 K in fields up to 14 T applied perpendicular to the wire. The irreversibility field H_{irr} was then approximated by linear extrapolation of the Kramer function $\Delta M^{0.5} H^{0.25}$–H plot to $\Delta M^{0.5} H^{0.25} = 0$, which defined the Kramer irreversibly field H_K. No geometric parameters were used in our Kramer function since we did not know the exact dimensions of the superconductor in the 5 mm section of wire, but the dimensions were the same for all samples investigated. The superconducting transition temperature T_c of these samples was determined using a Quantum Design 5 T SQUID magnetometer. The magnetic moment as a function of temperature was obtained by zero-field cooling the samples to 5 K, applying a 1 mT field parallel to the wire axis, and raising the temperature while measuring the magnetic moment.

3. Results

3.1. T_c and H_K

The SQUID T_c traces are nearly the same for all samples, with an onset T_c of 82 K and a broad transition ($\Delta T_c \approx 50$ K), indicative of the same oxygen doping in all samples [26]. H_K

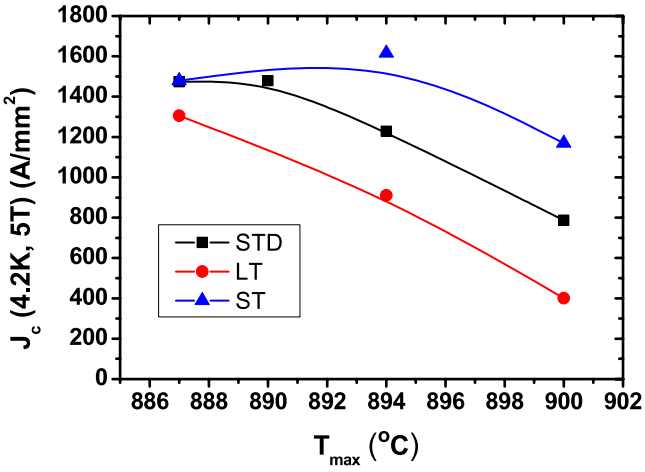

Figure 3. J_c (4.2 K, 5 T) as a function of T_{max} for fully-processed wires using STD, LT, and ST heat treatments. $t_{max} = 0.2$ h.

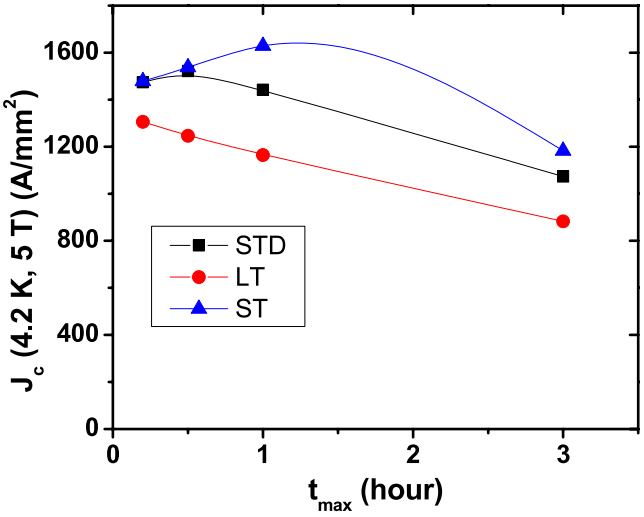

Figure 4. J_c (4.2 K, 5 T) as a function of t_{max} for fully-processed wire using STD, LT, and ST heat treatments. $T_{max} = 887$ °C.

(20 K) for all samples is ∼7.8 T, indicating that flux pinning, and therefore intragrain superconducting J_c, is essentially the same among all samples.

3.2. J_c and electromagnetic properties as a function of T_{max} and t_{max}

Figure 3 shows the transport J_c as a function of T_{max} for the three melt processing schedules. Raising T_{max} generally lowers J_c for all three schedules; however, at the same T_{max}, J_c varies significantly between schedules, particularly for higher T_{max}. For example, at $T_{max} = 894$ °C, J_c for STD and LT are 1228 and 909 A mm^{-2}, which are far lower than the 1620 A mm^{-2} for ST. It appears that the T_{max} windows are ∼887–890 °C for STD and ∼887–888 °C for LT, whereas for ST, the T_{max} window is ∼887–897 °C. Although at $T_{max} = 900$ °C, the J_c of ST decreases to 1170 A mm^{-2}; it is still 50% higher than J_c for STD and three times higher than J_c for LT.

Figure 4 presents J_c as a function of t_{max} for the three heat treatment schedules. $t_{max} > 1.5$ h generally leads to decreased J_c, but the exact J_c dependence on t_{max} is very different between the three heat treatment schedules. It appears that optimum t_{max} is ∼1.3 h for ST, ∼0.5 h for STD, and $\leqslant 0.2$ h for LT.

3.3. Microstructure as a function of T_{max}

We observed the phases present in the 2212 wires quenched at various points during the heat treatments. In one experiment, the samples were heated to T_{max} ranging from 887 to 905 °C, held for 0.2 h, and then quenched. The same phase mixture liquid plus two crystalline phases: alkaline earth cuprate ($(Sr, Ca)_{14}Cu_{24}O_x$, 14:24 AEC) and a copper-free phase ($(Bi_9(Sr, Ca)_{16}O_x$, 9:16 CF) was observed for all the samples, consistent with the oil-quenched Ag-sheathed 2212 tapes [27].

3.4. Microstructure as a function of t_{max}

Figure 5 presents microstructures of samples quenched after holding at $T_{max} = 887$ °C for various t_{max}. In this quench experiment $t_{melt} = t_{max} + \sim 2$ min $\cong t_{max}$. These images show that when melted, the filaments contain a mixture of liquid and crystalline phases plus gas-filled bubbles (pores) that are ∼20 μm in diameter and ∼50–200 μm long.

Immediately after melting (figure 5(a-1), $t_{max} = 0$ h), the filament architecture looked identical to that in the green wire. With increasing t_{melt}, the filaments bonded to adjacent filaments (figures 5(b) and (c)) and the filaments became fewer in number but larger in size as they agglomerated. After $t_{melt} =$ 48 h (figure 5(c), 48 h) there are few discrete filaments left and the bubbles have also become large as they have agglomerated together from multiple filaments. Figure 5 also shows a rather surprising result: the number and area of the AEC grains decreased with increasing t_{melt}. Quantitative microscopy using digital image analysis shows that the volume fraction of the AEC phase, calculated by the area ratio of AEC to filaments as determined from transverse cross-sections, decreased from ∼0.14 to ∼0.07 and its average grain size is nearly unchanged (∼75 μm^2) when increasing t_{melt} from 0.2 to 48 h. In contrast the grain size and volume fraction of the CF phase remain constant with increasing t_{melt} (average CF size ∼80 μm^2 and volume fraction of CF is ∼0.15).

3.5. J_c as a function of t_{melt}

Figure 6 shows J_c as a function of t_{melt}. This plot contains all the data for fully processed samples from the three types of heat treatments used in this study. It shows that J_c decreases approximately linearly with increasing t_{melt} when $t_{melt} \gtrsim 2.5$ h.

4. Discussion

Our goal in this study was to understand from a microstructural viewpoint what caused the wide variation in J_c that was attributed to using different T_{max} when heat treating 2212 round wire. These J_c–T_{max} windows ranged from as narrow as 2–4 °C up to 10 °C. We suspected that the time the sample is in the melt state has a critical effect on J_c, so we defined a

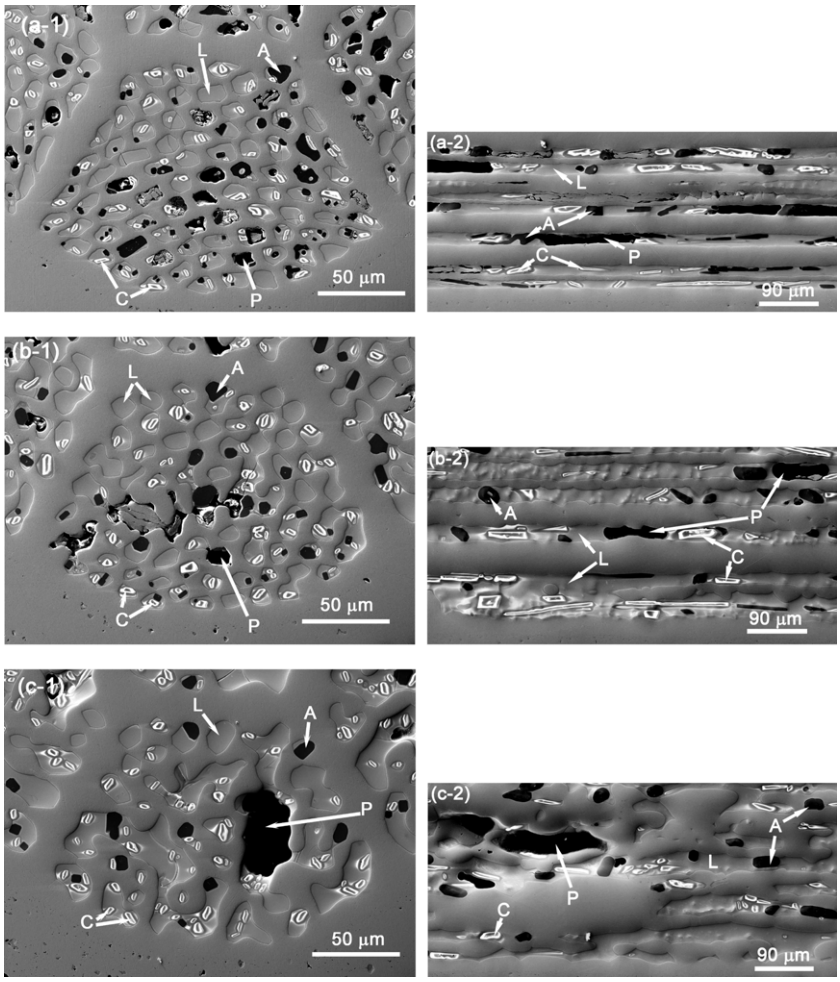

Figure 5. Secondary electron SEM micrographs of (1) transverse and (2) longitudinal sections of wires that were heated to $T_{max} = 887\,^{\circ}C$, held at 887 °C for various lengths of time (a) $t_{max} = 0$ h, (b) $t_{max} = 12$ h, and (c) $t_{max} = 48$ h and then quenched. For these samples, t_{melt} is t_{max}. The gray matrix is Ag, the black regions are 14:24 AEC or pores, the gray regions in the filaments are liquid, and the white particles are the Cu-free phase. A = AEC, C = Cu-free, P = pore, L = liquid. The bright contrast of the Cu-free particles is due to their insulating properties, which causes charging and increased secondary electron emission.

new processing variable t_{melt} (figure 1), and designed three heat treatments that changed t_{melt} while using the same T_{max} and t_{max}. We tried to design the three heat treatments so they were essentially the same, except for the melt region (figure 2). We think that changing the cooling rate in the melt state before 2212 begins to nucleate has very little effect on J_c; however, because we know that changing the cooling rate through the region where 2212 nucleates has a very large effect on J_c [23], we made sure the cooling rate when 2212 nucleates was the same for all three heat treatments. In addition, the three heat treatments were identical below 872 °C to room temperature, so processing conditions that can affect J_c in the latter stages of the heat treatment, such as oxygen uptake [26], were identical for all the samples. The following discussion shows that understanding the J_c–t_{melt} relationship holds the key to understanding why J_c often depends strongly on T_{max} and how this understanding can be used to develop heat treatment schedules that widen the T_{max} window.

The J_c–T_{max} data in figure 3 show the general trend that J_c decreases with increasing T_{max} above an optimum T_{max}. However, the data show a broad spread in J_c for a given T_{max} with different heat treatments. At $T_{max} = 900\,^{\circ}C$, J_c for the three heat treatment schedules varies by about a factor of 3. For ST, J_c shows a weak dependence on T_{max}: it decreases only by 25% when increasing T_{max} from 887 to 900 °C. Together these show that J_c only has a loose correlation with T_{max}.

We checked the phase assemblages in the melt in samples quenched from 887 and 905 °C to see if the decrease in J_c seen in figure 3 with increasing T_{max} might be due to having a different phase assemblage in the melt. The phase assemblages were the same and agreed with results from tape studies [27], showing that changes in phase assemblage cannot explain variations in J_c over this range of T_{max}.

The data in figure 4 show that J_c generally decreases with increasing t_{max} when $t_{max} > 1.5$ h, indicating that time at elevated temperature is an important variable that affects J_c. Figure 6 shows a better correlation between J_c and t_{melt} with J_c decreasing linearly with increasing t_{melt} for $t_{melt} \gtrsim 2.5$ h. There is a better correlation between J_c and t_{melt}, because, as we discussed in section 1, there is little difference in thermal energy over the T_{max} range we studied. This implies that all temperatures in the melt state are essentially equivalent, so

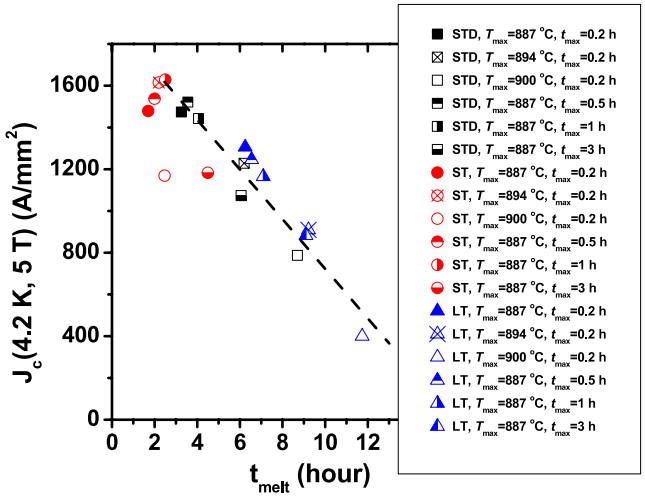

Figure 6. J_c (4.2 K, 5 T) as a function of t_{melt} for fully-processed wire using STD, LT, and ST heat treatments. J_c decreases linearly with increasing t_{melt} for $t_{melt} > 2.5$ h. The straight, dashed line is drawn as a guide to the eye. J_c increases from 0 A cm^{-2} at $t_{melt} = 0$ h, but we do not show an increasing trend line since we do not know what shape it should have.

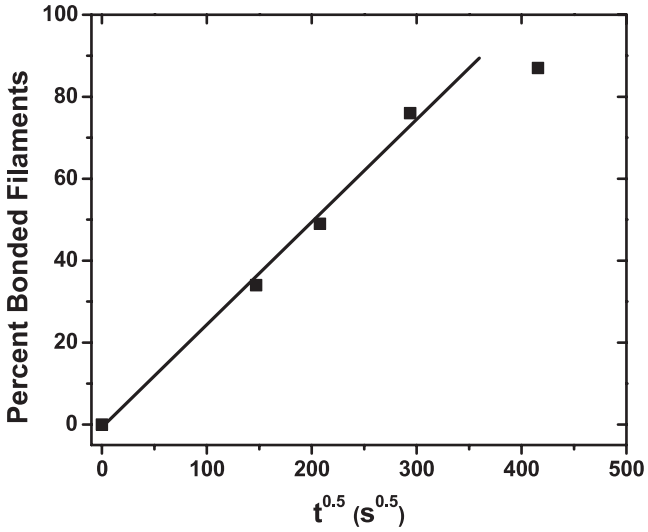

Figure 7. The per cent of bonded filaments as a function of $t_{melt}^{0.5}$. The linear increase in number of bonded filaments between 0 and 24 h indicates that filament bonding is a diffusion controlled process. The number of single filaments was determined from transverse cross-sectional micrographs of the wires from the experiment described and shown in figure 5.

the processes that occur in the melt state occur over the entire temperature range and are occurring during the entire time the sample is in the melt state. We defined t_{melt} to correspond to the total time in the melt state from 2212 melting to when 2212 begins to nucleate on cooling. However, we may actually be underestimating t_{melt} in this study because quench studies show that liquid is still present after 2212 nucleates and begins to grow. When t_{melt} is controlled to 1.7–2.5 h for the ST heat treatment, the T_{max} window can be widened to ∼10 °C (887–897 °C), within which J_c (4.2 K, 5 T) is >1475 A mm^{-2}. STD and LT showed narrow T_{max} windows (∼887–890 °C for STD and ∼887 °C for LT), most likely because samples stayed in the melt longer than necessary. For instance, $t_{melt} > 5.2$ h when $T_{max} > 890$ °C for STD ($t_{max} = 0.2$ h) and $t_{melt} > 6.6$ h when $T_{max} > 888$ °C for LT ($t_{max} = 0.2$ h).

The linear correlation between J_c and t_{melt} suggests that a steady state diffusion process is responsible for controlling J_c. Three processes occur when the wire is in the melt state that can affect 2212 grain connectivity. The first is filament bonding [23], which is seen in figure 5. Filament bonding, which occurs by a dissolution/diffusion/precipitation process, joins the filaments together in the melt state. Figure 5 shows graphically what happens to the filaments with increasing t_{melt}: filament bonding continues with increasing t_{melt} allowing the filaments in each bundle to merge into just a few large filaments (figure 5(c)). Figure 7 shows the per cent of bonded filaments as a function of $(t_{melt})^{1/2}$. The data from 0 to 24 h fall on a straight line indicating that filament bonding follows diffusion kinetics. Due to the continual liquid and Ag transport in the melt state, the initial, discrete filament structure collapses and the filaments merge, becoming much larger in diameter and distorted with increasing t_{melt}, as seen in figure 5(c). At some point, the effective filament diameters become much larger than the 2212 grain size, which means the filaments are too large to guide the 2212 grains to grow along the filament axis. The 2212 that forms in these large filaments is not well aligned along the filament axis, which decreases the connectivity and J_c.

We note that in figure 6, J_c is 0 A cm^{-2} at $t_{melt} = 0$ h, and increases up to the values shown in the figure with increasing t_{melt}. The data at short t_{melt} in figures 6 and 4 give some indication that J_c increases with increasing t_{melt} for the ST heat treatment. We speculate that this may be because when filament bonding occurs, large 2212 bridges can grow between the bonded filaments, increasing connectivity and J_c, as shown in [23]. At small t_{melt}, filament bonding creates 3D percolative pathways between filaments allowing the supercurrent to bypass non-superconducting second phases and bubbles in the porous 2212 wires. This portion of the J_c–t_{melt} plot needs to be studied in more detail. Because we do not know what shape the increasing trend line has, we have not drawn it in figure 6.

The second mechanism that occurs in the melt state that can decrease connectivity is bubble agglomeration in the filaments. Small bubbles that form when 2212 melts can agglomerate into larger, longer bubbles in individual filaments [28]. As discussed above, with increasing t_{melt}, the filaments bond together, which also allows bubbles in the bonded filaments to agglomerate into much larger bubbles that span multiple bonded filaments. The large bubble in figure 5(c) spans at least nine filaments. Kametani *et al* [29] and Jiang *et al* [30] have shown that bubbles decrease J_c, so we expect that large bubbles that span several bonded filaments are particularly potent current limiting defects since they block several bonded filaments simultaneously and they do not disappear during the heat treatment.

We speculate that the third process that decreases 2212 connectivity may be Cu loss from the melt. This is deduced from the surprising observation on the grain size and volume

fraction of the AEC and CF phases as a function of time. Quantitative analysis of the microstructures in the experiment shown in figure 5 showed that the volume fraction of the AEC grains decreased with increasing t_{melt}, whereas their average grain sizes did not change. The analysis also showed that the size and volume fraction of the CF grains did not change with increasing t_{melt}. These observations were unexpected since we anticipated the grain size of both of these phases would increase and their volume fraction would remain constant with increasing t_{melt}, as had been suggested in the literature [31]. Since the 14:24 AEC has the highest Cu concentration amongst the phases in the melt, this decrease in volume fraction of AEC indicates Cu is lost from the filaments with increasing t_{melt}.

Cu has the highest solubility and diffusivity in Ag among the BSCCO cations [32]. Before the present study we knew of three mechanisms by which Cu could be lost from the 2212 filaments. These are: (1) Cu dissolving into and saturating the Ag sheath, Majewski *et al* [33, 34] found a concentration of ∼0.5 at.% Cu in the Ag sheath equilibrated with 2212 at 860 °C in air; (2) Cu reacting with MgO (plus oxygen) in the Ag(Mg) outer sheath forming (Mg, Cu)O; and (3) Cu reacting with the alumino-silicate insulation surrounding the 2212 wire [32, 35]. The present study may suggest a fourth Cu loss mechanism, which is Cu evaporation, as an oxide, from the surface of the bare Ag sheath at elevated temperature. The Cu loss depletes the Cu content in the filaments, which shifts the overall 2212 composition and can result in less 2212 phase forming, which decreases J_c. The Cu loss also negatively impacts the nucleation and growth of 2212. We saw this when we quenched two wires that had significantly different t_{melt}. 2212 in the wire with the shorter t_{melt} nucleated at 872 °C as observed previously. In contrast 2212 in the wire with the longer t_{melt} nucleated as low as 860 °C (t_{melt} = 11.7 h). The Cu loss mechanism of copper oxide evaporating from the surface of the bare Ag sheath still needs to be confirmed experimentally.

There are two key findings from this study that have significant, positive impacts on heat treating coils. First is the observation that t_{melt} rather than T_{max} is the critical variable that leads to lower J_c at higher T_{max}. The second is the finding that by controlling t_{melt}, J_c is relatively insensitive to T_{max} over a much wider temperature range than had been suggested in the literature, which we found to be 10 °C from 887 to 897 °C. Together these indicate that it will be easier to heat treat large 2212 coils because by controlling t_{melt}, the T_{max} window can be widened. Controlling t_{melt} allows greater point-to-point temperature variations in the industrial furnaces used to process large coils than the (±1–2 °C) control that magnet builders envisioned being required to heat treat large 2212 coils.

5. Conclusions

We investigated the dependence of J_c of round Ag-sheathed 2212 wires on heat treatment conditions. We identified a new processing parameter, t_{melt}, which is the time in the melt defined as the time between when 2212 melts on heating and when 2212 begins to form on cooling. J_c decreases linearly with increasing t_{melt} when $t_{melt} > 2.5$ h. We could achieve high J_c over a wide T_{max} window (887–897 °C) using a heat treatment where we controlled t_{melt}. An important conclusion from this study is that it will not be necessary to have temperature uniformity of ±1–2 °C in large industrial furnaces to successfully heat treat 2212 coils. Instead high J_c can be achieved by controlling t_{melt}. We also probed the mechanisms that control J_c, finding three fundamental diffusion processes occurring in the melt that are important for determining the connectivity and J_c: (1) the filament dissolution/diffusion/precipitation process that bonds filaments together and alters the filament architecture, due to Ag and liquid transport in the melt; (2) bubble agglomeration where the bubbles that span several bonded filaments can form; (3) and possibly Cu loss from 2212 filaments. Although our observations are made on Ag-sheathed multifilamentary round wire, the importance of t_{melt} and these diffusion processes may also apply to other 2212 conductor forms.

Acknowledgments

Work at the NHMFL is supported by the NSF Cooperative Agreement DMR-0084173, by the State of Florida, and by an ARRA grant through the US Department of Energy. We would like to thank David Myers, Bill Starch, Van Griffin, and Natanette Craig for technical assistance with electromagnetic properties measurements and metallographic polishing and imaging. We thank the members of the Very High Field Superconducting Magnet Collaboration for helpful discussions.

References

[1] Miao H, Marken K R, Meinesz M, Czabaj B and Hong S 2005 *IEEE Trans. Appl. Supercond.* **15** 2554–7
[2] Schwartz J *et al* 2008 *IEEE Trans. Appl. Supercond.* **18** 70–81
[3] Godeke A *et al* 2008 *IEEE Trans. Appl. Supercond.* **18** 516–9
[4] Nachtrab W T, Renaud C V, Wong T, Liu X T, Shen T M, Trociewitz U P and Schwartz J 2008 *IEEE Trans. Appl. Supercond.* **18** 1184–7
[5] Hasegawa T *et al* 2001 *IEEE Trans. Appl. Supercond.* **11** 3034–7
[6] Trociewitz U P *et al* 2009 *Mag Lab Report* vol 16, pp 27–8
[7] Friend C M, Miao H, Huang Y, Melhem Z, Domptail F, Meinesz M, Hong S, Young E A and Yang Y 2010 *IEEE Trans. Appl. Supercond.* **20** 583
[8] Godeke A *et al* 2010 *Supercond. Sci. Technol.* **23** 034022
[9] Barzi E, Turrioni D, Miao H, Hong S, Kikuchi A, Lamm M, Marken K, Rusy A, Yamada R and Zlobin A V 2008 *Adv. Cryog. Eng.* **54** 431
[10] Heine K, Tenbrink J and Thoner M 1989 *Appl. Phys. Lett.* **55** 2441–3
[11] Shen T M, Liu X T, Trociewitz U P and Schwartz J 2008 *IEEE Trans. Appl. Supercond.* **18** 520–4
[12] Liu X T, Shen T M, Trociewitz U P and Schwartz J 2008 *IEEE Trans. Appl. Supercond.* **18** 1179–83
[13] Marken K R, Dai W, Cowey L, Ting S and Hong S 1997 *IEEE Trans. Appl. Supercond.* **7** 2211–4
[14] Kase J, Irisawa N, Morimoto T, Togano K, Kumakura H, Dietderich D R and Maeda H 1990 *Appl. Phys. Lett.* **56** 970–2
[15] Kase J, Morimoto T, Togano K, Kumakura H, Dietderich D R and Maeda H 1991 *IEEE Trans. Mag.* **27** 1254–7
[16] Lang T, Buhl D and Gauckler L J 1998 *Physica* C **294** 7–16

[17] Matsumoto A, Kitaguchi H, Kumakura H, Nishioka J and Hasegawa T 2004 *Supercond. Sci. Technol.* **17** 989
[18] Miao H, Marken K, Meinesz M, Czabaj B, Hong S, Rikel M O and Bock J 2006 *AIP Conf. Proc.* **824** 673
[19] Bruzek C E *et al* 2004 *6th European Conf. Applied Superconductivity*; *IOP Conf. Ser.* **181** 2260–7
[20] Rikel M O *et al* 2006 *J. Phys.: Conf. Ser.* **43** 51–4
[21] Holesinger T G, Baldonado P S, Van Vo N, Dai W M, Marken K R and Hong S 2009 *IEEE Trans. Appl. Supercond.* **9** 1800–3
[22] Weijers H W, Hu Q Y, Hascicek Y S, Godeke A, Vouchkov Y, Celik E, Schwartz J, Marken K, Dai W and Parrell J 1999 *IEEE Trans. Appl. Supercond.* **9** 563–6
[23] Shen T, Jiang J, Kametani F, Trociewitz U P, Larbalestier D C, Schwartz J and Hellstrom E E 2010 *Supercond. Sci. Technol.* **23** 025009
[24] Shen T 2010 *PhD Thesis* Florida State University
[25] Hellstrom E 1995 *High-temperature Superconducting Materials Science and Engineering: New Concepts and Technology* ed D L Shi (Oxford: Pergamon)
[26] Shen T, Jiang J, Yamamoto A, Trociewitz U P, Schwartz J, Hellstrom E E and Larbalestier D C 2009 *Appl. Phys. Lett.* **95** 152516
[27] Hellstrom E and Zhang W 1996 *Bismuth-Based High-Temperature Superconductors* ed H Maeda and K Togano (New York: Dekker)
[28] Scheuerlein C, Di Michiel M, Scheel M, Jiang J, Kametani F, Malagoli A, Hellstrom E E and Larbalestier D C 2011 *Supercond. Sci. Technol.* **24** 115004
[29] Kametani F, Shen T, Jiang J, Scheuerlein C, Di Michiel M, Huang Y, Miao H, Parrell J A, Hellstrom E E and Larbalestier D C 2011 *Supercond. Sci. Technol.* **24** 075009
[30] Jiang J, Starch W L, Hannion M, Kametani F, Trociewitz U P, Hellstrom E E and Larbalestier D C 2011 *Supercond. Sci. Technol.* **24** 082001
[31] Rikel M O, Wesolowski D, Yuan Y and Hellstrom E E 2001 *Physica* C **354** 321–6
[32] Wesolowski D E, Rikel M O, Jiang J, Arsac S and Hellstrom E E 2005 *Supercond. Sci. Technol.* **18** 934–43
[33] Majewski P, Aubele A, Fahr T and Aldinger F 1999 *Physica* C **325** 8–12
[34] Majewski P, Aubele A, Fahr T and Aldinger F 2001 *Physica* C **351** 62–66
[35] LoSchiavo M 2009 *MS Thesis* Florida State University